JOURNAL OF GEOPHYSICAL RESEARCH, VOL. 90, NO. D3, PAGES 5665–5675, JUNE 20, 1985

Linear Prediction of Sea Ice Anomalies

C. M. JOHNSON[1]

Max-Planck-Institut für Meteorologie, Hamburg, Federal Republic of Germany

P. LEMKE

Geophysical Fluid Dynamics Program, Princeton University, Princeton, New Jersey, and Max-Planck-Institut für Meteorologie, Hamburg, Federal Republic of Germany

T. P. BARNETT

Scripps Institution of Oceanography, La Jolla, California

Stationary and cyclostationary statistical models are developed to predict Arctic and Antarctic sea ice anomalies, using as predictors previous sea ice, atmospheric, and oceanic anomalies. A prediction model hierarchy is developed by using first internal (i.e., sea ice) predictors, including persistence, lateral advection, and diffusion, and a cyclostationary model that allows the prediction coefficients to vary seasonally. An external cyclostationary model hierarchy is developed next to investigate the ability of atmospheric winds, heat flux proxies, air temperatures, and sea surface temperatures (SST's) to predict sea ice extent. In the Arctic the highest skill was generally achieved by the cyclostationary internal model. Attempts to forecast the ice data at 1–2 month intervals after removal of its autoregressive component, using external predictors, gave nonsignificant models. At longer lead times (e.g., 3 months) the SST in the North Pacific was superior to persistence for sea ice prediction in the western Bering Sea. In the Southern Ocean, especially off East Antarctica, the model that included lateral advection and diffusion outperformed both persistence and the cyclostationary internal model. In the Weddel Sea and the Ross Sea, persistence proved to be the best sea ice predictor. No external models were tested for Antarctic sea ice because of insufficient data.

1. INTRODUCTION

This study is an attempt to ascertain how well one can predict sea ice anomalies at time scales of months to seasons. The main emphasis here will be on Arctic sea ice, since longer time series are available from this region. Improved prediction models of ice have become more important and necessary in recent years as a result of the increased volume of shipping in the Arctic and the recent discoveries of offshore oil in the Bering and Beaufort seas. Also physical and numerial models of sea ice point to the important role of this quantity in both the radiation and heat budgets in polar regions—and hence in global climate [*Untersteiner*, 1975].

In order to better understand the causes and effects of Arctic sea ice variability, a number of different types of models (dynamic, thermodynamic, stochastic, statistical, to name a few) has been developed to complement the increasing set of observational results. For instance, both dynamic and thermodynamic models have simulated, with reasonable success, the gross features of the Arctic pack ice [cf. *Parkinson and Washington*, 1979; *Thorndike et al.*, 1975; *Hibler*, 1980, *Stigebrandt*, 1981]. The stochastic methods of *Hasselmann* [1976] have been used by *Lemke et al.* [1980] to describe the statistical space-time structure of sea ice anomalies in terms of white noise atmospheric forcing, local stabilizing relaxation, and lateral diffusion and advection. On the observational side, such gross features as the average seasonal cycle of total Arctic sea ice area have been calculated by a number of authors in recent years [e.g., *Sanderson*, 1975; *Walsh and Johnson*, 1979*a*, hereafter WJ1; *Lemke et al.*, 1980].

Research on local ice forecasting has been an active area for scientific study. In a qualitative analysis of the Greenland-Northern European seesaw [*van Loon and Rogers*, 1978; *Rogers and van Loon*, 1979], unusually cold winters in Greenland and warm winters in Europe were often found to be followed by more than normal sea ice in the Davis Strait and less than normal ice in the Baltic Sea. These results are similar to those of *Vinje* [1975]. *Overland and Pease* [1982] found the externally forced variation of cyclone position to be the primary factor in determining interannual variability of sea ice extent in the Bering Sea, while *Rogers* [1978] found the cumulative number of thawing degree days occurring in spring to be one of the best predictors of the summertime ice extent off Barrow. A quantitative study of predictability by *Walsh* [1980] found persistence to be the best predictor of Alaskan sea ice extent on the order of months. Similar studies by *Walsh and Johnson* [1979*b*; hereafter WJ2] and by *Walsh and Sater* [1981; WS] found that persistence, sea surface temperature (SST) and surface air temperatures were sometimes effective predictors of sea ice extent.

What is missing in earlier ice prediction studies, however, is some sort of comprehensive treatment of all Arctic regions and a systematic comparison of atmospheric, oceanic, and sea ice predictors. Such a uniform approach to the sea ice forecast problem is one of the goals of this paper. In addition, the use of cyclostationary terms (e.g., seasonally varying prediction coefficients) in the modeling process [cf. *Hasselmann and Barnett*, 1981] offers a new, but logical, extension of WJ2, WS, and the stochastic model of *Lemke et al.* [1980]. The question to answer here is whether seasonally dependent prediction coefficients improve on the predictability, and if so, for which sectors and forecast intervals.

[1] Presently at The Artificial Intelligence Center, Siemens AG, Munich, Federal Republic of Germany.

Paper number 4D1194.
0148-0227/85/004D-1194$05.00

In overview the paper consists of a data description (section 2) followed by the linear forecasting techniques and model evaluations procedures (section 3). Section 4 discusses a hierarchy of forecast models with internal predictors, i.e., prediction of future sea ice extent, using previous sea ice data only. Section 5 describes the results of attempting to predict future ice variations with cyclostationary models using external predictors, i.e., previous atmospheric and oceanic data. Section 6 discusses teleconnections of sea ice and the Southern Oscillation Index. The conclusions and limitations of this study are summarized in section 7.

2. Data

The Arctic sea ice data set is based on 25 years (1953–1977) of monthly averaged ice-covered areas in 36,10° longitudinal sectors, as described by WJ1. The data were obtained from ship and aircraft measurements in the initial period; the last 11 years of data were satellite derived. In this study the Arctic sea ice data was actually used on a 30° longitudinal grid as indicated in Figure 1.

Due to this relatively large-scale as well as year-round approach to Arctic sea ice anomalies, certain deficiencies in the data (such as monthly averages substituted for missing data at individual grid points, particularly in the winter months and at the beginning of the study period—see WJ1) were not so crucial to the results presented here. However, this would not be the case for a more detailed, small-scale, and/or wintertime study of sea ice with this data, such as that done by *Overland and Pease* [1982].

Monthly near-surface atmospheric temperature and pressure fields for the same time period (1953–1977) were calculated from gridded northern hemispheric products of the National Meteorological Center. Monthly time series of sea surface temperature were created from the Surface Marine Deck (TDF11). The regions over which the atmospheric and oceanic fields were averaged to obtain specific predictor time series are shown in section 5.

The 8-year (1973–1981) Antarctic data of the sea ice edge (concentration larger than 5/8) on a 10° longitudinal grid is based on the weekly southern hemisphere sea ice charts published by the U.S. Fleet Weather Facility, Suitland, Maryland (for further detail, see *Lemke et al.* [1980]). In this study, only monthly averages of Southern Ocean sea ice data were used at four selected longitudes (Figure 1).

3. Linear Prediction Methods

The linear prediction models were constructed following the methods described in *Barnett and Hasselmann* [1979, BH] for systems with stationary statistics and as extended in *Hasselmann and Barnett* [1981, HB] to the cyclostationary case. The associated problems of determining model order and significance are discussed by *Barnett et al.* [1981]. The techniques used here are described briefly, since the above references develop the subject in detail.

The prediction models we shall be concerned with are the class of general cyclostationary, multilagged, multipredictor linear regression models of the form (cf. BH, HB)

$$y(t+q) = \sum_{i=0}^{m'} \sum_{l=0}^{m} D_{itl} x_i(t-l) + \eta(t) \qquad (1)$$

where y denotes the predictand, x_i the predictor set, q and l are (discrete) lead and lag times, respectively, and η is the residual, which is to be minimized. Both y and x_i are detrended, and the mean annual cycle is subtracted prior to use in the modeling process. The cyclostationarity is expressed by the dependence of the regression coefficient D_{itl} on time t and is assumed to be periodic:

$$D_{itl} = D_{i(t+p)l} = D_{ikl} \qquad (2)$$

where p is the period (in our case, 12 for monthly data) and $k = t(\text{mod } p)$. Thus, k represents a monthly index running from 0 to $p-1$.

The cyclostationary case can be reduced to the standard stationary case either by constructing separate models for each phase k of the annual cycle (fixed phase models) or by

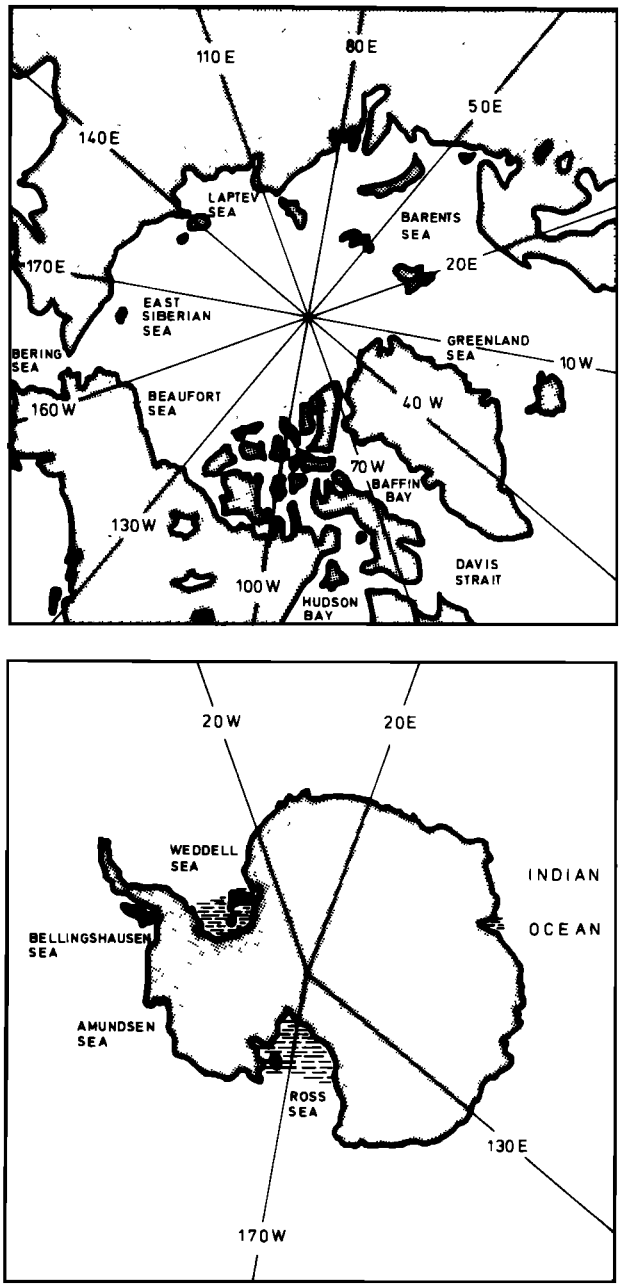

Fig. 1. Spatial distribution of sea ice predictor and predictand regions (sectors) for internal model hierarchy.

expanding the coefficients in a Fourier series

$$D_{ikl} = E_{il}^{0} + \left[E_{il}^{c} \cos \frac{2\pi k}{p} + E_{il}^{s} \sin \frac{2\pi k}{p}\right] + \left[E_{il}^{2c} \cos \frac{4\pi k}{p} + E_{il}^{2s} \sin \frac{4\pi k}{p}\right] + \cdots \quad (3)$$

and then optimizing the model simultaneously over the entire annual cycle (phase-averaged model).

If the Fourier expansion (3) is truncated below the Nyquist frequency, in this case 6 cpy, the phase-averaged model contains fewer coefficients and therefore generally achieves a higher statistical significance than a fixed phase model, i.e., a model that, in this case, has an explicit prediction coefficient for each month. On the other hand, if a statistically significant fixed-phase model can be constructed, it has the advantage of providing a full resolution of the annual cycle (cf. HB).

Truncating (3) at the first harmonic and substituting it into (1), the phase-averaged model may be written in the notation of a stationary, nonlagged regression model

$$y'(t+q) = \sum_{\gamma=1}^{n} a_\gamma' z_\gamma'(t) + \eta \quad (4)$$

where the a' are the prediction coefficients associated with a transformed, orthonormal predictor set (EOF's, z'), 'γ' represents a compression of the subscript triple shown in (3). With $y' = y/\langle y^2\rangle^{1/2}$, the prediction coefficients are given by

$$a_\gamma' = \langle y' z_\gamma' \rangle \quad (5)$$

Methods of determining the appropriate model order (n in (4)) and the statistical significance of the a_γ' are given in BH and *Barnett et al.* [1981]. The important quantities here are the hindcast skill, the artificial skill, and the ρ^2 statistic. The hindcast skill, being the fraction of the variance of y' that is explained by the model, is defined generally by

$$S_H = 1 - \frac{\langle (\Sigma_\gamma a_\gamma' z_\gamma')^2 \rangle - \langle y'^2 \rangle}{\langle y'^2 \rangle} \quad (6)$$

but reduces in the transformed coordinate system to

$$S_H = \sum_{\gamma=1}^{n} (a_\gamma')^2 \quad (7)$$

This paper considers only hindcasts, since all available data are used to determine the prediction coefficients (5).

In practice the hypothetical averages $\langle \cdots \rangle$ must be estimated from finite data samples. The sampling errors in the cross correlations introduce errors in the prediction coefficients a_i'

$$\delta a_i' = a_i' - a_i^{0} \quad (8)$$

and an apparent, or "artificial," skill given by

$$S_A = \sum_i \langle (\delta a_i')^2 \rangle \quad (9)$$

where a_i^{0} is the "true" value derived from a hypothetical infinite data ensemble, i.e., the artificial skill is the expected hindcast skill, assuming there is no real correlation between predictors and predictand $a_i^{0} = 0$.

The significance of a prediction model can then be expressed in terms of the statistic

$$\rho^2 = \sum_{ij} M_{ij}^{-1} \delta a_i' \delta a_j' \quad (10)$$

where $M_{ij} = \langle \delta a_i' \delta a_j' \rangle$. The calculation of the covariance matrix of the sampling errors M_{ij} is shown in the appendix of BH. The procedure used here is straightforward, as in BH, except for a slight modification of the significance test to include the effects of self-correlation, i.e., by retaining an additional series in the expression for the error covariance matrix (BH, equation (A3)). The aim of statistical prediction is to have $S_H \gg S_A$ and at the same time keep ρ^2 large enough to exceed the 95% confidence level of a zero prediction model (see BH). The latter criterion provides an objective method of determining the highest acceptable model order (n) in the hierarchy defined by (4).

Interpreting model results is an important aspect of the modeling process and is described in some detail in BH and in *Jenkins and Watts* [1968]. The basic idea in this study will be to discuss the important predictor-predictand relations through the transfer functions, i.e., the prediction coefficients E_{il}^{0}, E_{il}^{c} and E_{il}^{s} (equation (3)). These transfer functions are equivalent to the Green's functions of the differential equations that link the predictor and predictand and thereby provide information on the phase and time scales of the linkage.

4. INTERNAL PREDICTORS

The predictands and predictors considered for the Arctic are the ice-covered areas in 12, 30° longitudinal sectors (Figure 1). Since sea ice data is being used to predict future sea ice variations, we refer to the predictors as "internal." The 30° sectors were chosen so as to divide them into those bordering continents and those having access to a larger water body. These sectors also correspond to those used in *Johnson* [1980]. As predictands and predictors for the Antarctic we chose four typical 10° longitudinal sectors centered around 20°E, 130°E, 170°W, and 20°W (Figure 1). The predictor set also included the adjacent neighbor sectors immediately on each side of the predictand sector.

4.1. *Model Hierarchy*

A series of models was used to predict the behavior of each sector time series (the predictand). This model hierarchy is described briefly as follows:

Model 1. Simple persistence: Predictor 1 equals sea ice cover in the same sector as predictand.

Model 2. Neighbors: Predictor 1 equals sea ice cover in the same sector as predictand. Predictor 2 equals sea ice cover in eastern adjacent sector. Predictor 3 equals sea ice cover in western adjacent sector.

Model 3. Cyclostationary: Predictor 1 equals sea ice cover in the same sector as predictand. Predictor 2 equals predictor 1 multiplied with sin ($2\pi k/p$). Predictor 3 equals predictor 1 multiplied with cos ($2\pi k/p$).

Model 1 describes persistence, while model 2 allows for interaction with the eastern and western neighboring sectors. The transfer functions for the adjacent sectors can be interpreted as lateral advection and diffusion of sea ice anomalies [cf. *Lemke et al.*, 1980]. The cyclostationary model 3 may be thought of as periodic persistence. It allows the prediction coefficients to vary seasonally. All models are applied with one lag of prior information (i.e., $l = 0$ in equation (1)) for a variety of prediction lead times (q).

4.2. *Model Results: Arctic*

We will examine first hindcast skill versus sector at a fixed prediction lead time for the three models just discussed. The results for a lead time of 1 month are shown in Figure 2. The neighbor model does not appear to show much improvement

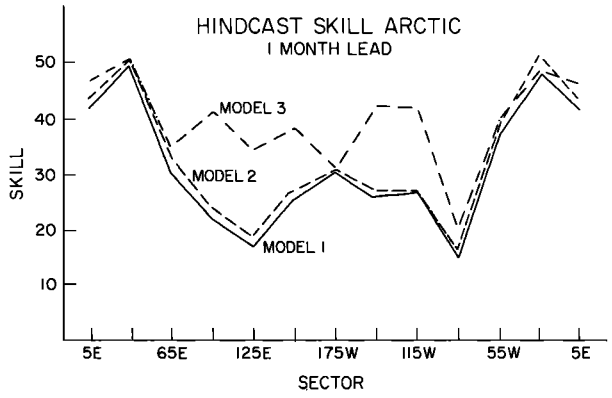

Fig. 2. Hindcast skill (%) versus sector for the internal Arctic model hierarchy. Lead time is 1 month. All values are significant.

over the persistence case. This is consistent with the results of *Lemke et al.* [1980], who found that, while advection processes were important for the Antarctic where continental infringement does not obstruct east-west ice transports, a more simple model without advection sufficed for the Arctic. The cyclostationary model shows improvement over the persistence approach for a number of sectors, the most marked being the Beaufort Sea (145°W) and the sector to the east (115°W). The differences in hindcast skill over the persistence model are also significant for both of these sectors [see *Johnson*, 1983, Table 4]. This tendency continues as one looks at the results for the predictands to the west. The difference between cyclostationary and persistence models becomes quite small in the Bering Sea (175°W), where wintertime variability is large. However, the model differences again become substantial in the Siberian Arctic (155°E to 95°E), where variability is again more or less restricted to summer. So the cyclostationary approach at short lead times appears to be most fruitful for predicting ice in those sectors blocked from further ice growth in winter by continents. Clearly, a prediction coefficient constant throughout the year does not well describe these latter situations. At this point one might look ahead and infer that a cyclostationary model may not prove as crucial in the Antarctic (see section 4.3).

The hindcast skill values versus longitude (sector) for a 3-month prediction lead time are shown in Figure 3. Note that a significant model could not be constructed for a number of sectors (open circles). Moreover, the more sophisticated models did not show a significant improvement over the simple persistence model. Although the only significant model

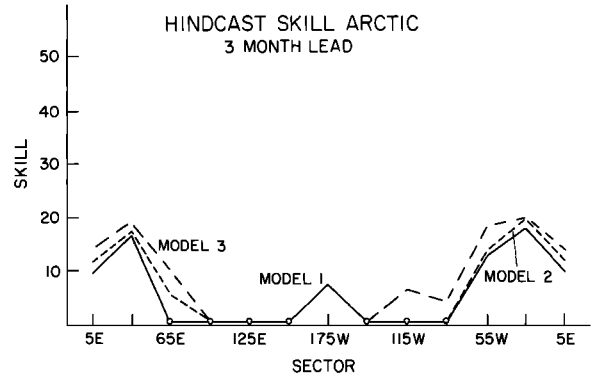

Fig. 3. Same as Figure 2, but for lead time of 3 months. The open circles indicate nonsignificant values.

TABLE 1. Hindcast Skill Versus Lead Time for the Model Hierarchy Applied to the East Siberian Sea

Model	Lead Time, months	S_H, %	S_A, %
1	1	26	1
	2	3	1
	3	—	—
2	1	27	2
	2	3	1
	3	—	—
3	1	38	2
	2	9	2
	3	—	—

at a 3-month lead time for some sectors (again those with limited wintertime variability) was the cyclostationary one, the improvement over persistence was not as dramatic as for the 1-month lead time.

Two sectors were chosen to test skill versus prediction lead time: East Siberian Sea (155°E) and the Barents Sea (35°E). The Siberian sector has a small lagged autocorrelation, while the Barents Sea has a higher one. The hindcast skill and significance for lead times of 1–6 months was computed for both sectors.

None of the models were found to be significant beyond a lead time of 2 months in the Siberian sector (Table 1). This is possibly due to the poor quality of the data from this region (see WJ1). The cyclostationary model does not show much improvement for prediction lead times of 3 months or more, and that is not surprising: The basic predictability of the system (based on internal factors) has also already dropped well below significance at 3 months. At lead times of 1 or 2 months though, the increase in hindcast skill of the cyclostationary model over persistence (see Table 1) does seem real.

The results of hindcast skill versus lead time for the Barents sector are shown in Table 2. The simple persistence model shows apparent skill out to a 5-month lead time. Expectedly, the neighbors and cyclostationary models are significant up to a prediction lead of 6 months. However, these models show little increase in hindcast skill over persistence for lead times up to 5 months. It is only at the 6-month lead time that the

TABLE 2. Hindcast Skill Versus Lead Time for the Model Hierarchy Applied to the Barents Sea

Model	Lead Time, months	S_H, %	S_A, %
1	1	49	2
	2	32	2
	3	17	2
	4	10	2
	5	7	2
	6	—	—
2	1	50	3
	2	32	3
	3	17	3
	4	11	3
	5	12	3
	6	9	3
3	1	50	3
	2	33	3
	3	19	3
	4	12	3
	5	11	3
	6	13	3

higher-order models become appreciably different from simple persistence.

Comparing these results with those from the Siberian sector, one can make the following remarks concerning the improvement of the cyclostationary model over simple persistence: For sectors with a small autocorrelation time, e.g., East Siberian Sea, the cyclostationary model appears to show improvements primarily at smaller prediction lead times. For sectors with greater persistence (e.g., Barents Sea, Denmark Strait) the cyclostationary model may only show improvement at larger lead times or act to increase the maximum forecast interval.

The above studies were generalized to examine the limit (in time) of predictability versus sector. The maximum forecast interval for each sector is shown in Figure 4. The corresponding skill values and number of significant predictors are given in Table 6 of *Johnson* [1983]. The Barents Sea (35°E) sector shows the highest significant maximum forecast interval within the model hierarchy considered here. This is not surprising, since the Barents sector also has one of the highest autocorrelations at a 1-month lag.

It is interesting to note that neither the "neighbors" nor the cyclostationary models increased the maximum forecast interval for those sectors in the Siberian and Alaskan Arctic (95°E to 145°W). The maximum forecast interval in the Eurasian Arctic (35°E to 65°E) can be increased on the order of 1 month by either cyclostationary or neighbor models. The largest increase in maximum prediction interval from a more complex model, however, is shown for the cyclostationary approach in the Canadian Arctic, including Baffin Bay (115°W to 55°W). Of these latter sectors, two tend to have little wintertime variability (Victoria Island and Hudson Bay), although this is not the case for Baffin Bay.

The dependence of the hindcast skill on seasonal phase was investigated next for several selected regions. It was found that the skill was generally positive in the winter and summer months but negative during the advance and retreat phase in fall and spring, respectively. The reason for the negative skill was investigated by constructing a fixed-phase model for each month, i.e., fully resolving the annual cycle. This latter model showed substantial hindcast skill in winter and summer, with low values in spring and fall. This may be because the winter/-summer steady state ice conditions simply last for a relatively long time, while the transition between seasonal states is fairly

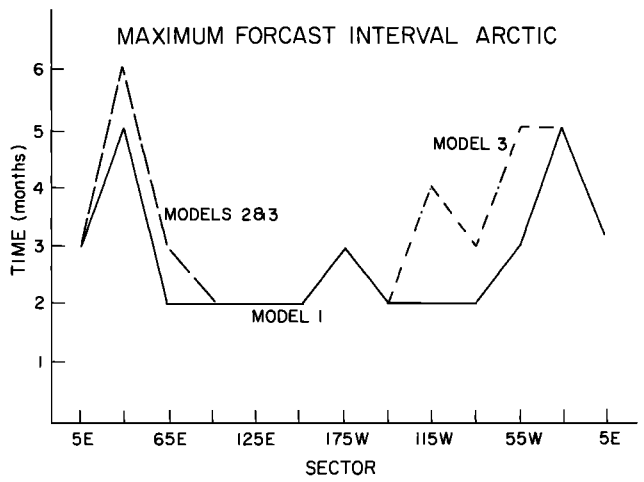

Fig. 4. Maximum significant forecasts interval versus sector for the internal Arctic model hierarchy.

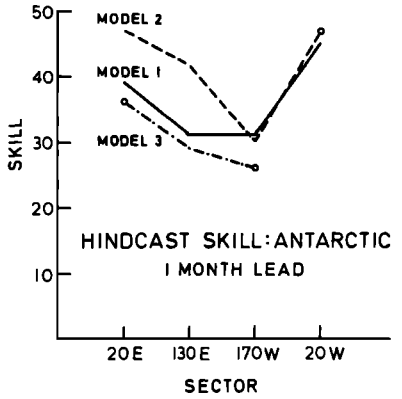

Fig. 5. Hindcast skill (%) versus sector for the internal Antarctic model hierarchy. Lead time is 1 month. Open circles indicate 90% instead of 95% significance.

rapid. This distribution of prediction coefficients suggests that for practical prediction purposes it will be necessary to retain higher-order harmonics in the Fourier expansion (equation (3)).

4.3. *Model Results: Antarctic*

Due to the short time series of Antarctic sea ice (8 years), estimation errors in the prediction coefficients become relatively large, increasing the artificial skill S_A and decreasing the significance ρ^2. Therefore it is generally more difficult to create acceptable models for the Southern Ocean sea ice. The results of the application of the model hierarchy to 10° sectors centered at various longitudes around Antarctica demonstrate this fact (Figure 5 and Table 3).

Although the hindcast skill was relatively large, the higher-order models generally failed to be significant at 95% for prediction leads of 2 months and more (Table 3). Only the persistence model was able to predict sea ice anomalies for up to 2-month lead times. This short maximum forecast interval is partly due to the shortness of the sea ice time series. However, it is also in accordance with the short correlation time scale of Antarctic sea ice, which is of the order of 1 to 2 months compared to 1 to 4 months for Arctic sea ice. The maximum forecast interval for the persistence model at 20°E and 130°E (1 month) and at 170°W and 20°W (2 months) is in

TABLE 3. Hindcast Skill for the Model Hierarchy Applied to Various Antarctic Sectors

Sector	Model	Lead Time, months	S_H, %	S_A, %
20°E	1	1	39	2
	2	1	47	7
		2	(16)	(4)
	3	1	(36)	(5)
130°E	1	1	31	2
	2	1	42	7
	3	1	29	5
170°W	1	1	31	2
		2	11	2
	2	1	30	5
	3	1	(26)	(5)
20°W	1	1	45	4
		2	22	4
	2	1	(47)	(10)
	3	1	—	—

The parentheses indicate models that were only significant at the 90% level.

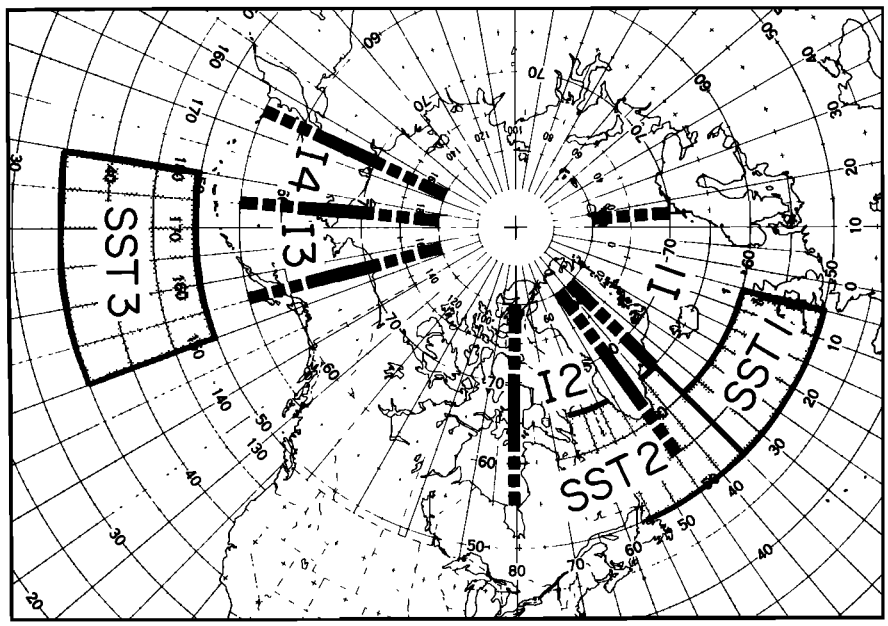

Fig. 6. Spatial distribution of sea ice predictand regions (I1 through I4) and SST predictor regions (SST1 through SST3) for external model hierarchy.

accord with the autocorrelation time scale of sea ice anomalies at those longitudes [cf. *Lemke et al.*, 1980].

At 20°E and 130°E the Antarctic Circumpolar Current and the prevailing westerlies affect the evolution of sea ice anomalies throughout most of the year. Model 2 (neighbors) generally yielded a larger skill than persistence (model 1) and the cyclostationary model 3, which at 20°E was only significant at the 90% level (Figure 5). In the Ross Sea (170°W), persistence and neighbor models performed equally well for 1-month leads, while model 3 was only significant at the 90% level. For a 2-month prediction lead time, both higher-order models failed the significance test. In the Weddell Sea (20°W), persistence seems to be the only acceptable model. Although its skill was high (47%), the neighbor model was only valid at 90%.

Generally, the seasonal modulation of the prediction coefficients did not prove to be important for Antarctic sea ice anomalies in contrast to the Arctic. Advection and diffusion, on the other hand, seem to be significant for the Southern Ocean sea ice. The transfer coefficients of model 2 agree with the observed and empirically determined [cf. *Lemke et al.*, 1980] advection pattern of Antarctic sea ice.

The seasonal dependence of hindcast skill for the Antarctic

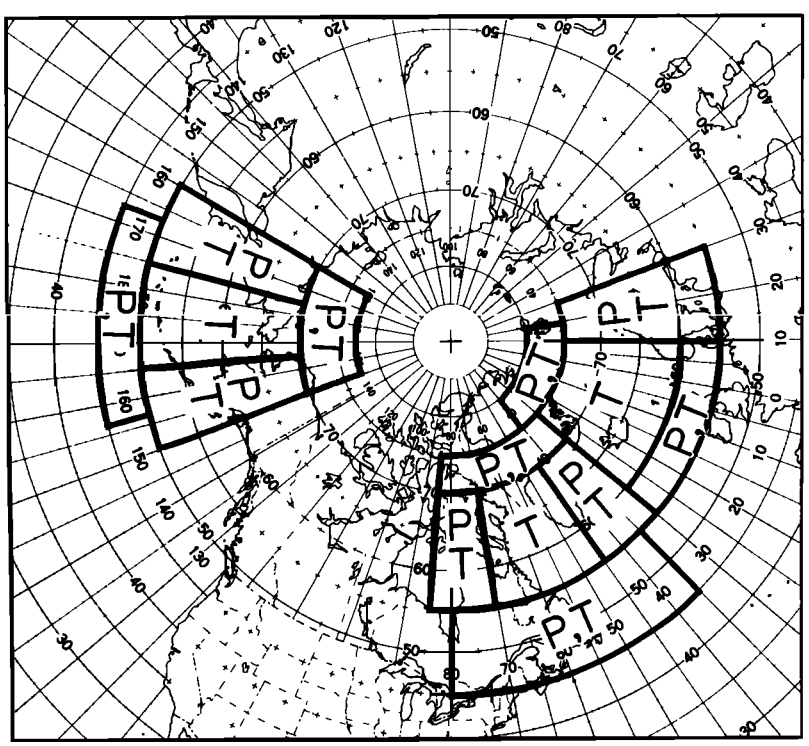

Fig. 7. Spatial distribution of atmospheric predictor regions (p, sea level pressure; T, 1000–700 mbar thickness) for external model hierarchy.

appeared similar to the situation in the Arctic. Both cyclostationary and full-resolution fixed-phase models suggest higher-order annual harmonics in the hindcast skill. The short Antarctic data series made a quantitative description of this signal highly uncertain.

5. EXTERNAL PREDICTORS

Recent investigations of large-scale interactions in the sea ice–ocean–atmosphere system have shown that the Arctic sea ice extent is contemporaneously correlated with the high-latitude atmospheric circulation patterns and SST distributions [e.g., *Walsh and Sater*, 1981; *Walsh and Johnson*, 1979*b*; *Crane*, 1978; *Overland and Pease*, 1981; *Niebauer*, 1980; *Schell*, 1970]. The usefulness of these cross correlations for large-scale, long-term, and seasonally dependent prediction of sea ice extent has not generally been established in previous studies (for an exception, see *Walsh* [1980]). The emphasis in this section, then, is to investigate the predictive skill of a hierarchy of seasonally dependent prediction models that utilize as predictors atmospheric and oceanic variables, which will be called henceforth "external" predictors.

These models are applied to several selected sectors of Arctic sea ice as shown in Figure 6. One set of external predictors is the sea level pressure fields (P) surrounding each ice sector such that east-west and north-south pressure gradients will represent the v and u components of the atmospheric geostrophic flow over the sector, respectively (Figure 7). The air temperature predictors (T) are taken here as proportional to the 1000–700 mbar thickness (Figure 7). These predictors and their spatial gradients were used to represent mean atmospheric temperatures and atmospheric heat fluxes over the sectors. In our analysis the sea surface temperature information is also investigated. The regions over which these predictors (SST1, SST2, SST3) were averaged are also shown in Figure 6. All predictors and predictands were detrended, and the annual cycle was subtracted.

5.1. *Model Hierarchy*

The model hierarchy for atmospheric and oceanic data used to forecast the sea ice in a specific sector is characterized as follows:

Model 1: Predictors 1–4 equal the four sea level pressure (SLP) predictors that surround the sector.

Model 1: Predictor 1 equals the sum of all atmospheric pressure fields that surround the sector. Predictor 2 equals east-west pressure difference (v component of geostrophic flow in atmosphere). Predictor 3 equals north-south pressure difference (u component of geostrophic flow in atmosphere).

Model 3: Predictor 1 equals east-west pressure difference (meridional wind component) multiplied with north-south temperature difference (equal to meridional atmospheric heat flux). Predictor 2 equals north-south pressure difference (zonal wind component) multiplied with east-west temperature difference (equal to zonal atmospheric heat flux).

Model 4: Predictor 1 and 2 as in model 3. Predictor 3 equals air temperature above the ice sector.

Model 5: Predictors 1–3 as in model 4. Predictor 4 equals sea surface temperature in designated area.

Unless stated otherwise, all predictors are applied with two lags (i.e., $l = 0$ and 1 in equation (1)) for a variety of lead times (q). Note that the maximum n in (4) is 6 times the number of atmospheric and oceanic predictors stated above for each model. A factor of 2 arises from the two time lags applied, and a factor of 3 is due to the first three Fourier coefficients used in the expansion of the prediction coefficients (3), i.e., for model 5, $n_{max} = 24$. The complete set of predictors for each model is orthogonalized, and only the results for the first six or ten EOF's are displayed in the following figures.

5.2. *Model Results*

This section summarizes the results of applying the above model hierarchy to a selected group of regional Arctic sea ice data.

Davis Strait. The results of the model hierarchy applied to the Davis Strait sector (I2) for a 1-month prediction lead time are shown in Figure 8. Generally, skill and significance increase with increasing model number. The best model is model 5, although it is only marginally better than model 4. This is due to the poor correlation between the Davis Strait sea ice and SST2, which lies downstream of the major ocean current, the Labrador Current. *Walsh and Sater* [1981] also found rather small correlations between sea ice and SST in the North Atlantic, whereas large correlations were found for North Pacific SST and Bering Sea ice. The best predictor in model 5 is the east-west atmospheric heat flux, followed by the air temperature above the ice sector, the north-south atmospheric heat flux, and finally the SST2.

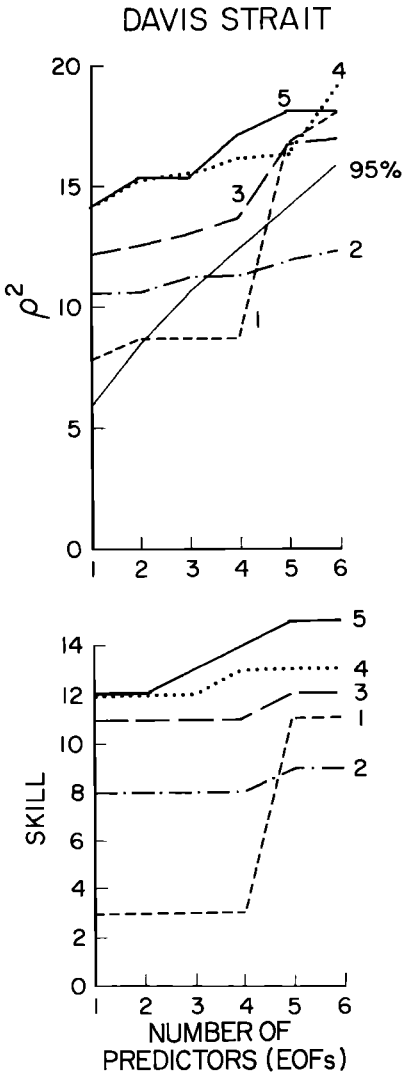

Fig. 8. Significance ρ^2 and skill S_H (%) for the external Arctic model hierarchy applied to the Davis Strait sector (I2). Lead time is 1 month. The lags are 0 and 1 month.

The decomposition of the skill into monthly values (seasonal skill) shows that the prediction of sea ice anomalies with external predictors is far better in winter than in summer, when the skill levels are practically zero. This feature is characteristic of all models (Figure 9). The seasonal skill of the internal models introduced in section 4, on the other hand, exhibits large positive values for both winter and summer and large negative values during the advance and retreat phase in fall and spring, respectively.

Adding 1 year of past prediction information into model 5, as opposed to only the last 2 months, did not significantly change ρ^2, S_H, and its seasonal dependence. The transfer functions (i.e., prediction coefficients) drop off to small values for lags larger than 3 months (Figure 10), thereby explaining this result. Increasing the prediction lead time shows that model 5 can predict sea ice anomalies in the Davis Strait for up to 3 months ahead (Figure 11). Predicting sea ice with its own past values (persistence) generally yields larger values for ρ^2 and S_H (see Figures 2 and 3). If persistence is removed from the sea ice time series, none of the above models is valid to describe the residuals.

Bering Sea. The results of the model hierarchy for a 1-month prediction interval applied to the western Bering Sea (I4) are shown in Table 4. As in the Davis Strait, model 5 provides the best prediction in the western Bering Sea, especially if 1 year of past information is used in the predictor set. The main new result here is that the Pacific SST3 is more important as a predictor for western Bering Sea ice. This is demonstrated in Figure 12. Whereas the transfer functions for the atmospheric predictors drop off to smaller values for lags larger than 2 or 3 months, it remains significant for the Pacific SST3 throughout the past year. The increase of the transfer function for the air temperature at lags of 9 to 11 months suggests that a low-frequency signal is present in both the air temperature and the sea ice time series.

The best predictor in model 5 (with 1 year of past information) is the Pacific SST3, followed by the air temperature above the sea ice, the meridional atmospheric heat flux, and finally the zonal heat flux. As in the Davis Strait the seasonal skill is large in winter and small in summer. Increasing lead time shows that model 5 can predict sea ice anomalies significantly for up to 3 months ahead (Figure 13). The hindcast skill for the best significant "external" model ($S_H = 25\%$) for a 1-month prediction interval is slightly smaller than that for the best "internal" model (30.5%, see Figure 2). For a 3-month prediction interval the best "external" model (15%) is better than the best "internal" model (7%, see Figure 3).

In the eastern Bering Sea (I3), the Pacific SST3 is of no help as a predictor. Indeed, the maximum forecast interval is only 1 month. At that short time scale the best predictors are the air

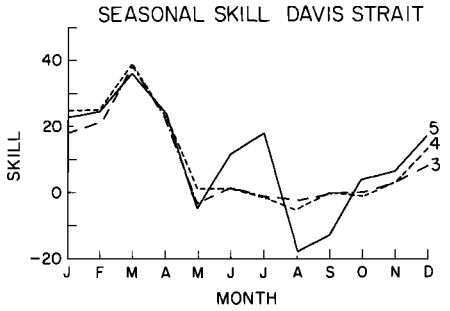

Fig. 9. Seasonal skill (%) for models 3, 4, and 5 applied to the Davis Strait (I2). Lead time is 1 month. The lags are 0 and 1 month.

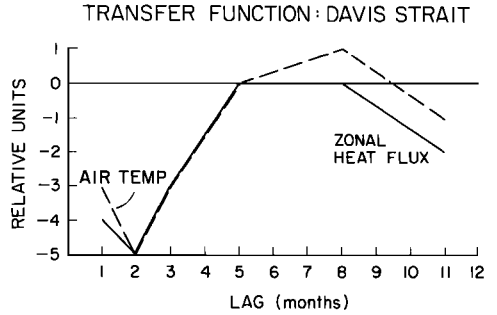

Fig. 10. Transfer functions (equal to prediction coefficients) for the zeroth Fourier coefficient of the zonal heat flux (solid line) and air temperature (dashed line) as a function of lag time from model 5 applied to the Davis Strait (I2).

temperature above the ice sector, followed by the north-south atmospheric heat flux, the east-west atmospheric heat flux, and finally by the Pacific SST3. The skill is only significant from February to May and is negligible during the rest of the year.

Greenland Sea. The results of the model hierarchy applied to the Greenland Sea sector (I1) for 1-month lead and 2-months lag time are given in Table 5. Generally, the skill was a factor of 2 smaller than for the other sectors. Models 3 and 4 were not acceptable, models 1 and 2 only at the 90% confidence level. The best predictor in model 2 was the meridional wind.

The only model accepted at the 95% level was model 5, but the skill of 6% was not impressive. The seasonal distribution of the skill showed large values (14% and 27%) for November and December and was practically zero throughout the rest of the year. The best predictor of model 5 was the air temperature, followed by the meridional heat flux and SST1. No significant model was achieved for 2 or more months prediction lead times. Increasing the lag time did not improve the model performance.

6. Teleconnections

The coupling between the tropical regions of the globe and higher latitudes is a subject of much current research. We undertook a cursory examination of possible couplings between climate variations in the tropics, represented here by the Southern Oscillation Index (SOI), and the variability of sea ice in sectors 1–4 (see Figure 6) and also for the Barents Sea. The results presented below suggest the need for additional effort

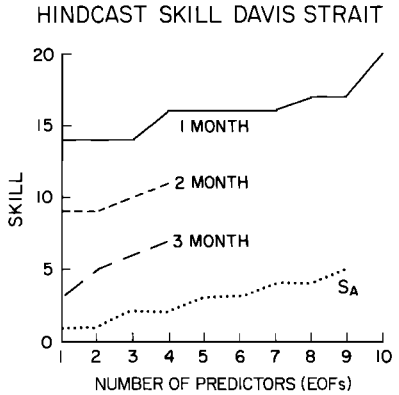

Fig. 11. Hindcast skill (%) for different lead times for model 5 applied to the Davis Strait (I2). The truncation of the curves denotes the significance cutoff.

TABLE 4. Hindcast Skill for the Model Hierarchy Applied to the Western Bering Sea (I5) for 1-Month Lead and 2-Month Lag Times

Model	S_H, %	S_A, %
1	3	1
2	—	—
3	11	2
4	12	2
5	14	3
5*	25	7

Model 5 was also applied with 12 months lag time (*).

to study what appears to be potentially real, tropical-high latitude couplings.

6.1. *Methods*

The SOI, defined here as the SLP difference between Easter Island and Darwin, was available at monthly intervals for the period of the ice record (1957–1977). Possible SOI/sea ice couplings were investigated with the time-dependent cross-correlation function, i.e.,

$$r(m, \tau) = \langle I(m, v) \cdot S(m, v, \tau) \rangle_v$$

where I and S represent the monthly sea ice and SOI time series respectively, m is a month counter (1, 2, ..., 12), v is a year counter (1957, 1958, ..., 1977), and τ is a time lag (-6, -5, ..., 5, 6 months). Significance levels on r were determined according to *Jenkins and Watts* [1968], after taking account of the autocorrelated natures of I and S. As a rule of thumb, $r \geq 0.4$ is expected to occur by chance less than 10% of the time if I and S are uncorrelated.

6.2. *Results*

The relation between two sea ice sectors and the SOI were selected for discussion. The other ice sectors follow one or the other of these two, as noted.

Greenland Sea (I1). The time-dependent correlation between the SOI and Greenland Sea series is shown in Figure 14 (upper). Much the same picture emerged for the Barents Sea sector. It is clear that the nature of the SOI in early summer gives a hint as to the subsequent summer and winter's sea ice condition in the Greenland Sea. The size of the correlation suggests predictive skill levels of 15%–20%; values typically as large as those found in sections 4 and 5. The correlations

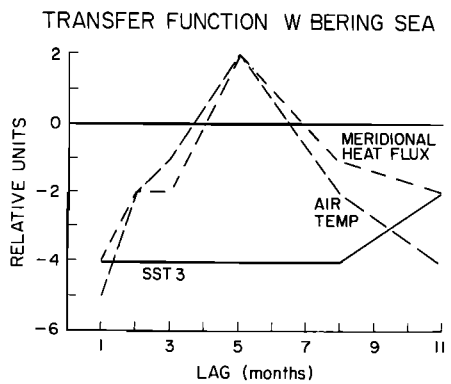

Fig. 12. Transfer functions (equal to prediction coefficients) for the zeroth Fourier coefficient of SST3 (solid line), the air temperature (dashed line), and the meridional heat flux (dashed-dotted line) as a function of lag time from model 5 applied to the western Bering Sea (I4).

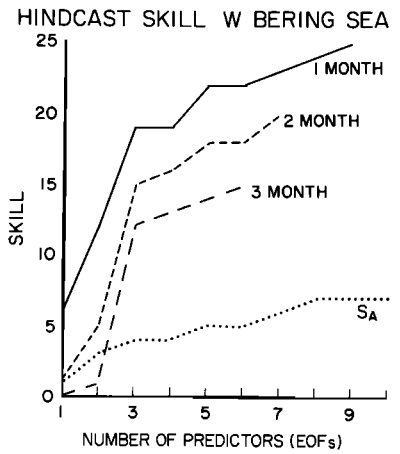

Fig. 13. Hindcast skill (%) for different lead times for model 5 applied to the western Bering Sea (I4). The truncation of the curves denotes the significance cutoff.

are positive, so high SOI in June, say, leads to heavy sea ice in the fall/winter.

The other main feature on the upper panel is the large area of negative correlation between SOI in the fall and subsequent sea ice behavior in the early spring. In this case a high SOI in fall will lead to rather light sea ice concentration in the following spring. The size of the correlation (~0.4) suggests predictive skill of 16%; the models of sections 4 and 5 did not possess this level of skill at the implied 4-month lead times.

Western Bering Sea (I4). The time-dependent correlation (Figure 14, lower) shows two significant features, features that are generally shared by the eastern Bering Sea and Davis Strait sectors. The first is a "negatively correlated" structure relating fall SOI and subsequent sea ice concentrations (as found for the Greenland Sea). The sense of the relation is the same: high SOI equals low sea ice. But the predictive lead time is now much less, being of order 0–2 months, while the skills are higher, ranging to 20%–30%. Apparently the SOI/-sea ice conditions are more closely and strongly linked in time than ice conditions farther removed from the SO region of influence.

Perhaps the most interesting result is seen in the upper left and right quadrants of Figure 14 (lower). Relatively large (> 0.4), negative correlations suggest that winter-spring sea ice conditions can be used to predict subsequent SOI variations in the spring-summer seasons. Less sea ice would suggest future high SOI values. The implied skill level of 10%–25% is appreciable.

6.3. *Discussion*

Although the relations shown in Figure 14 are marginally significant, they seem unlikely to be statistical artifacts, since

TABLE 5. Hindcast Skill for the Model Hierarchy Applied to the Greenland Sea (I1) for 1-Month Lead and 2-Month Lag Times

Model	S_H, %	S_A, %
1	(4)	(1)
2	(5)	(2)
3	—	—
4	—	—
5	6	1

Parentheses indicate models that were only acceptable at the 90% level.

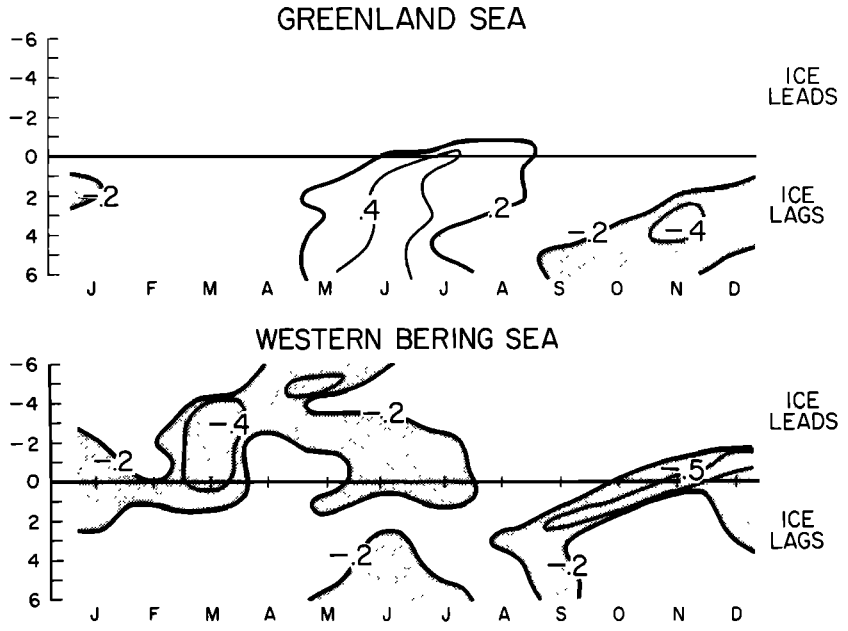

Fig. 14. Seasonally dependent cross correlation between the Southern Oscillation Index and sea ice extent in the Denmark Strait (upper panel) and the western Bering Sea (lower panel). Stipped regions denote negative correlations. Values exceeding 0.40 are significant at the 90% level. The time lag (months) is shown on the ordinate.

the regions of significant cross correlation form a pronounced pattern and are not randomly distributed. The explanation of this pattern is beyond the scope of this paper. However, *Walker and Bliss* [1932], *Berlage* [1966], *Horel and Wallace* [1981], and *Wallace and Gutzler* [1981], among others, have shown clear teleconnections between the SOI and the higher-latitude circulation features of the northern hemisphere. In a sense, then, the results of Figure 14 are not unexpected. However, the sharp seasonality of the relations, if real, must be explained.

The suggestion that ice conditions might be used to predict SOI seems relatively new. However, before this possibility can be seriously considered it will be necessary to develop a physical rationale to support what is otherwise an intriguing, but purely statistical, relation.

7. Conclusions

The application of an autoregressive model hierarchy to Arctic sea ice shows that the cyclostationary model improves upon simple persistence in most sectors, especially those sectors with limited wintertime variability (due to continental infringement) and for shorter forecast intervals. The inclusion of "neighbor interaction" with adjacent sectors provides little increase in true skill, consistent with the findings of *Lemke et al.* [1980]. For Antarctic sea ice the neighbor model generally outperforms persistence or the cyclostationary model, except for the Weddell and the Ross Sea, where persistence seems to be more significant. This result is again in accord with the findings of *Lemke et al.* [1980].

The model hierarchy that used external (i.e., nonice) predictors generally achieved smaller skill than the internal model hierarchy. The exceptions to this conclusion occurred in the western Bering Sea, where the North Pacific SST provides a better prediction than the sea ice itself for 3 months lead. No single external predictor could consistently explain most of the predictive skill, although air temperature over the predictand sea ice sector was the most consistent performer. Heat flux in the atmosphere was the second best predictor set on average, but the relative roles of the meridional and zonal fluxes were not well defined.

Removal of simple persistence from the Arctic sea ice sector data left a residual that generally differed little from "white noise." All external models failed to predict the residuals in this case. Physically, this suggests that the stochastic dynamic model of sea ice proposed by *Lemke et al.* [1980] is consistent with the results of this study. For practical purposes this result suggests the simplest ice forecasting scheme (simple persistence) is relatively good. Improvements can be obtained by cyclostationary persistence models in areas of land infringement and through the introduction of external predictors (especially the SST) in the western Bering Sea. For Antarctic sea ice the inclusion of sea ice information in neighboring sectors seems to be more important than the introduction of cyclostationary terms.

A brief investigation of the relation between sea ice variation and the Southern Oscillation Index gave results that suggest strong couplings between the tropics and the Arctic region. No explanation for these apparent couplings is offered here, but the implied relationship looks secure enough to suggest future research into the matter.

Acknowledgments. This work was partially supported by the Office for Climate Dynamics of the National Science Foundation under contract ATM821327 (TPB), by the Max Planck Institute for Meteorology (CMJ, PL), and the Geophysical Fluid Dynamics Program, Princeton University/NOAA, grant 04-7-022-44017 (PL). Thanks are due K. Brennecke for programming aid and K. Hasselmann for informative discussions.

References

Barnett, T. P., and K. Hasselmann, Techniques of linear prediction, with application to oceanic and atmospheric fields in the tropical Pacific, *Rev. Geophys. Space Phys.*, *17*(5), 949–968, 1979.

Barnett, T. P., R. W. Preisendorfer, L. M. Goldstein, and K. Hasselmann, Significance tests for regression model hierarchies, *J. Phys. Oceanogr.*, *11*(8), 1150–1154, 1981.

Berlage, H. P., The Southern Oscillation and world weather, *Meded. Verh. 88*, 152 pp., K. Ned. Meteorol. Inst., Amsterdam, 1966.

Crane, R. G., Seasonal variations of sea ice extent in the Davis Strait-Labrador Sea area and relationships with synoptic-scale atmospheric circulation, *Arctic*, *31*, 434–447, 1978.

Hasselmann, K., Stochastic climate models, 1, Theory, *Tellus*, *28*, 473–485, 1976.

Hasselmann, K., Linear statistical models, *Dyn. Atmos. Oceans*, *3*, 501–521, 1979.

Hasselmann, K., and T. P. Barnett, Techniques of linear prediction for systems with periodic statistics, *J. Atmos. Sci.*, *38*, 2275–2283, 1981.

Hibler, W. D. III, Modeling a variable thickness sea ice cover, *Mon. Weather Rev.*, *108*, 1943–1973, 1980.

Horel, J. D., and J. M. Wallace, Planetary-scale atmospheric phenomena associated with the Southern Oscillation, *Mon. Weather Rev.*, *109*, 813–829, 1981.

Jenkins, G. M., and D. G. Watts, *Spectral Analysis and Its Applications*, 525 pp., Holden-Day, San Francisco, Calif., 1968.

Johnson, C. M., Wintertime Arctic sea ice extremes and the simultaneous atmospheric circulation, *Mon. Weather Rev.*, *108*, 1782–1791, 1980.

Johnson, C. M., A cyclostationary linear prediction model of Arctic sea ice, Hamburger Geophysikalische Einzelschriften, *Heft 62, Reihe A*, Wittenborn, Hamburg, 1983.

Lemke, P., E. W. Trinkl, and K. Hasselmann, Stochastic dynamic analysis of polar sea ice variability, *J. Phys. Oceanogr.*, *10*, 2100–2120, 1980.

Niebauer, J., Sea ice and temperature variability in the eastern Bering Sea and the relation to atmospheric fluctuations, *J. Geophys. Res.*, *85*, 7507–7516, 1980.

Overland, T. E., and C. H. Pease, Cyclone climatology of the Bering Sea and its relation to sea ice extent, *Mon. Weather Rev.*, *110*, 5–13, 1982.

Parkinson, C. L., and W. M. Washington, A large-scale numerical model of sea ice, *J. Geophys. Res.*, *84*, 311–337, 1979.

Rogers, J. C., Meteorological factors affecting interannual variability of summertime ice extent in the Beaufort Sea, *Mon. Weather Rev.*, *106*, 890–897, 1978.

Rogers, J. C., and H. van Loon, The seesaw in winter temperatures between Greenland and northern Europe, 1, Sea ice, sea surface temperatures, and winds, *Mon. Weather Rev.*, *107*, 509–519, 1979.

Sanderson, R. M., Changes in the area of Arctic sea ice, 1966 to 1974, *Meteorol. Mag.*, *104*, 313–323, 1975.

Schell, I. J., Arctic ice and sea temperature anomalies in the northeastern North Atlantic and their significance for seasonal foreshadowing locally and to the eastward, *Mon. Weather Rev.*, *98*, 833–850, 1970.

Stigebrandt, A., A model for the thickness and salinity of the upper layer in the Arctic Ocean and the relationship between the ice thickness and some external parameters, *J. Phys. Oceanogr.*, *11*, 1407–1422, 1981.

Thorndike, A. S., D. A. Rothrock, G. A. Maykut, and R. Colony, The thickness distribution of sea ice, *J. Geophys. Res.*, *80*, 4501–4513, 1975.

Untersteiner, N., Sea ice and ice sheets and their role in climatic variations, The Physical Basis of Climate and Climate Modelling, *GARP Bull. Ser. 16*, pp. 206–224, Global Atmos. Res. Proj., Geneva, 1975.

van Loon, H., and J. C. Rogers, The seesaw in winter temperatures between Greenland and northern Europe, 1, General description, *Mon. Weather Rev.*, *106*, 296–309, 1978.

Vinje, T. E., Sea ice conditions in the European sector of the marginal seas of the Arctic, 1966–1975, *Arbok, Norsk Polarinst.*, 163–174, 1975.

Walker, E. W., and G. T. Bliss, World weather, *V. Mem. R. Meteorol. Soc.*, *4*, 53–84, 1932.

Wallace, J. M., and D. S. Gutzler, 1981: Teleconnections in the geopotential height field during the Northern Hemisphere winter, *Mon. Weather Rev.*, *109*, 784–812.

Walsh, J. E., Empirical orthogonal functions and the statistical predictability of sea ice extent, in *Sea Ice Processes and Models*, edited by R. S. Pritchard, University of Washington Press, Seattle, 1980.

Walsh, J. E., and C. M. Johnson, An analysis of Arctic sea ice fluctuations, 1953–1977, *J. Phys. Oceanogr.*, *9*, 580–591, 1979*a*.

Walsh, J. E., and C. M. Johnson, Interannual atmospheric variability and associated fluctuations in Arctic sea ice extent, *J. Geophys. Res.*, *84*, 6915–6928, 1979*b*.

Walsh, J. E., and J. E. Sater, Monthly and seasonal variability in the ocean-ice-atmosphere systems of the North Pacific and the North Atlantic, *J. Geophys. Res.*, *86*, 7425–7445, 1981.

T. P. Barnett, Scripps Institution of Oceanography, La Jolla, CA 92093.

C. M. Johnson, The Artificial Intelligence Center, Siemens AG, Otto-Hahn Ring 6, 8000 Munich 83, Federal Republic of Germany.

P. Lemke, Max-Planck-Institut für Meteorologie, Bundestrasse 55, 2000 Hamburg 13, Federal Republic of Germany.

(Received March 19, 1984;
revised August 29, 1984;
accepted September 5, 1984.)